J. Fluid Mech. (1981), *vol.* 110, *pp.* 161–170
Printed in Great Britain

Stratified flow over a bounded obstacle in a channel of finite height

By G. S. JANOWITZ

Department of Marine Science and Engineering,
North Carolina State University, Raleigh, NC 27650

(Received 3 June 1980 and in revised form 23 September 1980)

The steady-state solution for the stratified flow over a bounded obstacle in a channel of finite height is obtained through the use of the inviscid unsteady Oseen equations; the body streamline encloses and is produced by a planar momentum sink. The calculations are compared with the experimental observations of Wei, Kao & Pao (1975) and Baines (1977). In a case where theoretical and experimental values match, good agreement was found. This suggests that the Oseen model with its columnar, wavelike and decaying solutions may provide a reasonable alternative to Long's model for subcritical flows.

1. Introduction

The study of stably stratified flows over obstacles has engaged the attention of fluid mechanicians over the past several decades, because of the geophysical importance of such flows as well as the challenges they pose to theoreticians and experimentalists alike. Many theoretical studies have been based on the use of Long's (1955) model for the steady two-dimensional inviscid stratified flow over obstacles. This model requires that in the steady state the density far upstream decreases linearly with height, $d\rho/dz = -\rho_0 N^2/g$, and that the kinetic energy per unit volume far upstream is independent of height. Under these conditions a linear Helmholtz equation for displacement function may be obtained without requiring that the obstacle be small. When an obstacle is towed with speed U through a linearly stratified fluid in a channel of height D and $\pi U/ND > 1$, these conditions are approximately satisfied and calculations based on Long's model are in good agreement with observations. For these supercritical flows, internal gravity waves cannot propagate upstream during the transient period prior to the establishment of a steady-state flow and the upstream requirements imposed by Long's model are not invalidated. However, for subcritical flows, $\pi U/ND < 1$, the upstream conditions may be changed due to the possibility of upstream propagation of internal waves during the transient period and the upstream conditions required by Long's model may not hold. Indeed, recent observations by Wei *et al.* (1975) and Baines (1977) have indicated that columnar disturbances, i.e. those independent of the distance upstream, do exist and because of their presence Long's model results yield poor quantitative agreement with his experimental evidence.

The analytical alternative to Long's model is the use of an Oseen model. Janowitz (1968) used this model to determine the disturbance due to a line momentum sink in an unbounded viscous flow. Trustrum (1971) used the unsteady inviscid Oseen

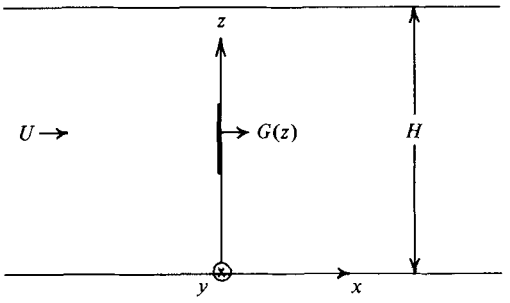

FIGURE 1. Geometry of the flow.

equations to compute the flow due to a vertical flat plate in a channel of finite height and Wong & Kao (1970) utilized the unsteady inviscid Oseen equations to study the disturbance caused by a line source of volume flux; this calculation led to a body shape unbounded in the downstream direction.

Our objective here is to use the inviscid unsteady Oseen equations to generate a steady-state solution for the flow past a smooth bounded obstacle in a channel of finite height and to compare these results with available observations. The utility of the Oseen approach will be demonstrated.

2. Specification and solution of the model

We consider an initially uniform flow of speed U with density $\rho = \rho_0(1 - N^2 z/g)$ in a channel of height H, see figure 1. A planar sink of x-momentum located in the y, z plane and independent of y is slowly turned on and we shall calculate the ensuing inviscid motion subject to Boussinesq and Oseen approximations. The governing equations are as follows:

$$\rho_0 \mathscr{L} u = -\partial p/\partial x + G(x, z, t), \tag{1}$$

$$\rho_0 \mathscr{L} w = -\partial p/\partial z - \rho g, \tag{2}$$

$$\mathscr{L}\rho = \rho_0 N^2 w/g, \quad \frac{\partial u}{\partial x} + \frac{\partial w}{\partial z} = 0, \tag{3), (4}$$

where

$$G(x, z, t) = F(z)\,\delta(x)\,e^{\epsilon t}, \tag{5}$$

and

$$\mathscr{L} \equiv \frac{\partial}{\partial t} + U\frac{\partial}{\partial x}. \tag{6}$$

Here u, w, p, and ρ are disturbances to the initial state and G is the force/(unit volume) in the x direction imposed upon the flow; it vanishes as $t \to -\infty$ and is gradually turned on thereafter. This technique was utilized by Lighthill (1965) to satisfy the radiation condition without employing a Laplace-transform technique. When the formal solution is determined we will let $\epsilon = 0$ to obtain the steady-state disturbance. The function $F(z)$ is the force per unit width per unit height and $\delta(x)$ indicates that the force is localized in the y, z plane.

We introduce a stream function as follows:

$$u = -\frac{\partial \psi}{\partial z}, \quad w = \frac{\partial \psi}{\partial x}. \tag{7}$$

A vorticity equation involving ρ and ψ is now obtained by cross-differentiating equations (1) and (2) to eliminate p. When the $\mathscr{L}$ operator is applied to the vorticity equation and equation (3) is utilized we obtain the following equation governing ψ:

$$\mathscr{L}^2\nabla^2\psi + N^2\frac{\partial^2\psi}{\partial x^2} = -\frac{1}{\rho_0}\mathscr{L}\frac{\partial G}{\partial z}, \tag{8}$$

where

$$\nabla^2 = \frac{\partial^2}{\partial x^2} + \frac{\partial^2}{\partial z^2}.$$

We now expand dF/dz in a Fourier sine series and seek solutions for ψ as follows:

$$\frac{dF}{dz} = \sum_{n=1}^{\infty} F_n \sin(n\pi z/H), \tag{9a}$$

$$\psi = e^{\epsilon t}\sum_{n=1}^{\infty}\psi_n(x)\sin(n\pi z/H), \tag{9b}$$

where

$$\psi_n = \frac{1}{(2\pi)^{\frac{1}{2}}}\int_{-\infty}^{+\infty}\phi_n(l)\,e^{ilx}\,dl. \tag{9c}$$

When equations (9) are substituted into equations (8), we obtain the following expression for $\psi_n(x)$:

$$\psi_n(x) = \frac{F_n}{2\pi\rho_0}\int_{-\infty}^{+\infty}\frac{-(il+\epsilon)\,e^{ilx}\,dl}{(Ul-i\epsilon)^2\,(l^2+(n\pi/H)^2)-N^2l^2}. \tag{10}$$

The integral can be evaluated by the method of residues. This integral is virtually identical to that evaluated by Lighthill (1967) in his discussion of an obstacle moving along the axis of a rotating fluid and we shall not repeat his discussion here. We let

$$\mathscr{K} = NH/\pi U$$

and M be the integral part of K,
i.e.

$$M \leqslant \mathscr{K} < M+1;$$

with these definitions, the steady-state solution for ψ, with ϵ now taken to be 0, is as follows. For $x \leqslant 0$,

$$\psi = \frac{U}{2\rho_0 N^2}\left[\sum_{n=1}^{M}\frac{\mathscr{K}F_n\sin(n\pi z/H)}{n(1-n/\mathscr{K})} + \sum_{n=M+1}^{\infty}\frac{F_n\sin(n\pi z/H)\exp(\tilde{\alpha}_n x)}{(n/\mathscr{K})^2-1}\right]. \tag{11a}$$

For $x \geqslant 0$,

$$\psi = \frac{U}{2\rho_0 N^2}\left[\sum_{n=1}^{M}\frac{\mathscr{K}F_n\sin(n\pi z/H)}{n(1+n/\mathscr{K})}\left\{1+\frac{2(n/\mathscr{K})}{1-n/\mathscr{K}}\cos\tilde{\alpha}_n x\right\} + \sum_{n=M+1}^{\infty}\frac{F_n\sin(n\pi z/H)}{(n/\mathscr{K})^2-1}\{2-\exp(-\tilde{\alpha}_n x)\}\right]. \tag{11b}$$

In the above

$$\tilde{\alpha}_n = (|(n/\mathscr{K})^2-1|)^{\frac{1}{2}}\mathscr{K}\pi/H. \tag{11c}$$

We note that both ψ and ψ_x are continuous across $x=0$, but ψ_{xx} and hence u_{xx} are not.

In previous work by the author (Janowitz 1974), the disturbances due to line singularities in unbounded stratified flow were investigated. The existence of upstream columnar disturbances was found to depend on the nature of the singularity; if either

u or u_{xx} were discontinuous across the singularity, then upstream columnar disturbances existed. This occurs here for the momentum sink singularity (u_{xx} is discontinuous). However, if only u_x is discontinuous, which was found to be the case for dipole and vortex singularities, no upstream columnar disturbances was found. We shall see that body shapes produced by the momentum sink singularity tend to be streamlined while those produced by a dipole (Janowitz 1974) tend to be more blunt. Thus body shape may have an influence on upstream influence.

We now limit ourselves to obstacles which are symmetric top to bottom and whose axis is located at $z = \frac{1}{2}H$. This is equivalent to an obstacle located at the bottom of a channel of height $\frac{1}{2}H$. We therefore let $F(z)$ be an even function of $(z-\frac{1}{2}H)$ and dF/dz will be an odd function of $(z-\frac{1}{2}H)$. With these limitations all the terms in (11a, b) with n an odd integer will vanish. For this case of an obstacle on the bottom of a channel of height $\frac{1}{2}H$, we make the following definitions:

$$\left.\begin{aligned} D &= \tfrac{1}{2}H, \quad K = \tfrac{1}{2}\mathscr{K} = ND/\pi U, \quad \eta = x/D, \\ \zeta &= (z-D)/D \quad (0 \leqslant \zeta \leqslant 1), \\ G_m &\equiv \frac{2}{D}\int_0^1 \frac{dF}{d\zeta}\sin(m\pi\zeta)\,d\zeta, \\ \alpha_m &= (|(m/K)^2-1|)^{\frac{1}{2}}K\pi \end{aligned}\right\} \tag{12}$$

and $\bar{K} \leqslant K < \bar{K}+1$, with $\bar{K}$ an integer or zero. For the symmetric or bottom towed obstacle, when $\eta \leqslant 0$,

$$\psi = \frac{U}{2\rho_0 N^2}\left[\sum_{m=1}^{\bar{K}} \frac{KG_m \sin(m\pi\zeta)}{m(1-m/K)} + \sum_{m=\bar{K}+1}^{\infty} \frac{G_m \sin(m\pi\zeta)}{(m/K)^2-1}\exp(\alpha_m\eta)\right]. \tag{13a}$$

When $\eta \geqslant 0$

$$\psi = \frac{U}{2\rho_0 N^2}\left[\sum_{m=1}^{K} \frac{KG_m \sin(m\pi\zeta)}{m(1+m/K)}\left\{1+\frac{2(m/K)}{1-m/K}\cos(\alpha_m\eta)\right\} + \sum_{m=\bar{K}+1}^{\infty} \frac{G_m \sin(m\pi\zeta)}{(m/K)^2-1}\{2-\exp(-\alpha_m\eta)\}\right]. \tag{13b}$$

In the following section we consider the disturbance due to a specific vertical force distribution.

3. A specific force distribution and its constraints

The results embodied in equations (13) are still quite general and to proceed to comparisons with experimental results we must specify $F(\zeta)$. We now take

$$\left.\begin{aligned} F(\zeta) &= -\frac{3\mathscr{D}}{4\rho_0 D}\frac{(\beta^2-\zeta^2)}{\beta^3}, \quad 0 \leqslant \zeta \leqslant \beta < 1, \\ &= 0, \quad \beta \leqslant \zeta \leqslant 1. \end{aligned}\right\} \tag{14}$$

Here $\mathscr{D}$ is the total drag force per unit width of a symmetric obstacle. We can readily show that

$$G_m = \frac{3\mathscr{D}}{\rho_0\beta^3 D^2\pi^2 m^2}\{\sin(m\pi\beta) - m\pi\beta\cos(m\pi\beta)\}. \tag{15}$$

We now let

$$\left.\begin{aligned} \tilde{\psi} &= \psi/UD, \quad C \equiv \frac{3}{2\pi^4}\frac{\mathscr{D}}{\rho_0 U^2\beta^2 D^2}, \\ \gamma_m &= \sin(m\pi\beta) - m\pi\beta\cos(m\pi\beta). \end{aligned}\right\} \tag{16}$$

The final form for $\tilde{\psi}$ is as follows. For $\eta \leqslant 0$

$$\tilde{\psi} = \frac{C}{K^2}\left[\sum_{m=1}^{K}\frac{K\gamma_m \sin(m\pi\zeta)}{m^3(1-m/K)} + \sum_{m=\bar{K}+1}^{\infty}\frac{\gamma_m \sin(m\pi\zeta)\, e^{\alpha_m\eta}}{m^2((m/K)^2-1)}\right]. \tag{17a}$$

For $\eta \geqslant 0$

$$\tilde{\psi} = \frac{C}{K^2}\left[\sum_{m=1}^{\bar{K}}\frac{K\gamma_m \sin(m\pi\zeta)}{m^3(1+m/K)}\left\{1+\frac{2(m/K)\cos(\alpha_m\eta)}{1-m/K}\right\} + \sum_{m=\bar{K}+1}^{\infty}\frac{\gamma_m \sin m\pi\zeta}{m^2((m/K)^2-1)}(2-e^{-\alpha_m\eta})\right]. \tag{17b}$$

In order to determine the values of C and β which yield body ($-\zeta+\tilde{\psi}=0$) streamlines which enclose the force distribution and are closed in both upstream and downstream directions we proceed as follows. We first fix K and consider values of $\beta = 0{\cdot}1$, $0{\cdot}2$, $0{\cdot}3$, $0{\cdot}4$, $0{\cdot}5$. We fix β and let $C = 1$ and compute $\psi_1 \equiv \tilde{\psi}(\eta, \zeta, K, C, \beta)|_{c=1}$. The body streamline will enclose the force distribution if, for $\eta = 0$, $0 \leqslant \zeta \leqslant \beta$,

$$-\zeta + C\psi_1(0,\zeta) \geqslant 0.$$

The minimum value for C is given by the maximum value of $\zeta/\psi_1(0,\zeta)$ at $\eta = 0$, $0 \leqslant \zeta \leqslant \beta$. The upstream horizontal velocity disturbance is negative for $\zeta < \beta$. For the body to be closed in the upstream direction, one maximum value for C is set by the requirement that, as $\eta \to -\infty$, $1 - C\,\partial\psi_1(\eta,0)/\partial\zeta > 0$. If the body streamline is closed on the downstream side it must be closed at $\alpha_k\eta = \pi$ as $\tilde{\psi}$ is most negative there. Therefore a second condition on the maximum value of C is set by the requirement that $-\zeta + C_1\psi_1(\pi/\alpha_{\bar{K}}, \zeta) < 0$ as $\zeta \to 0$. The maximum value for C with K and β fixed is the smaller of the two values required to close the streamline in upstream and downstream directions. With the procedure for determining the range of parameters now set we proceed to a discussion of our results and data comparisons in the next section.

4. Discussion of the results

Using the procedure outlined in the previous section, we considered values of $K = 1{\cdot}11$, $1{\cdot}25$, $1{\cdot}43$, $1{\cdot}60$, $1{\cdot}67$, $1{\cdot}80$, $1{\cdot}90$, $2{\cdot}22$ and $2{\cdot}50$ with β ranging from $0{\cdot}1$ to $0{\cdot}5$. For $K = 1{\cdot}6$, $1{\cdot}67$, $1{\cdot}80$ and $1{\cdot}90$ no values of C which produced closed streamlines could be found. For the other values of K, only certain values of β had acceptable ranges for C. With the acceptable combinations determined, the total dimensionless stream function ($-\zeta+\tilde{\psi}(\eta,\zeta)$) was computed on a rectangular grid. The dimensionless height (h) and length (L) of the obstacle as well as its shape was then determined as was the streamline pattern. Two typical body shapes are shown in figure 2. The strength of the columnar disturbance is characterized by the far upstream dimensionless horizontal velocity disturbance. For cases when $\bar{K} = 1$, only one mode exists upstream and we let $U_1 \equiv -\partial\tilde{\psi}(-\infty, 1)/\partial\zeta$. For cases when $\bar{K} = 2$, we define

$$U_2 = -\partial\tilde{\psi}(-\infty, \tfrac{1}{2})/\partial\zeta \quad \text{and} \quad U_1 \equiv -\partial\tilde{\psi}(-\infty, 1)/\partial\zeta + U_2.$$

K	B	C	h	L	h/L	U_1	U_2	U_1/h	U_2/h	C_D
1·11	0·1	2·40	0·140	1·10	0·130	0·694	—	4·96	—	1·13
1·11	0·1	2·65	0·167	1·23	0·136	0·767	—	4·59	—	1·03
1·11	0·1	2·90	0·195	1·37	0·142	0·839	—	4·30	—	0·97
1·11	0·1	3·15	0·223	1·46	0·153	0·912	—	4·09	—	0·92
1·11	0·2	0·407	0·227	0·91	0·249	0·915	—	4·03	—	0·93
1·11	0·2	0·419	0·238	0·96	0·247	0·941	—	3·91	—	0·91
1·11	0·1	3·40	0·253	1·72	0·147	0·984	—	3·89	—	0·87
1·11	0·2	0·443	0·260	1·30	0·200	0·995	—	3·83	—	0·88
1·25	0·2	0·740	0·230	0·958	0·240	0·739	—	3·21	—	1·67
1·25	0·2	0·760	0·236	0·984	0·240	0·759	—	3·22	—	1·67
1·25	0·2	0·990	0·304	1·18	0·258	0·989	—	3·25	—	1·69
1·43	0·3	0·450	0·315	1·21	0·260	0·841	—	2·67	—	2·50
1·43	0·3	0·470	0·323	1·34	0·241	0·879	—	2·72	—	2·56
2·22	0·1	2·50	0·122	0·655	0·186	0·066	0·702	0·539	5·75	1·33
2·50	0·2	0·90	0·207	0·978	0·211	0·150	0·796	0·725	3·85	2·26

TABLE 1. Summary of input parameters (K, B, C) and results. See text for definitions of h, L, U_1, U_2, C_D.

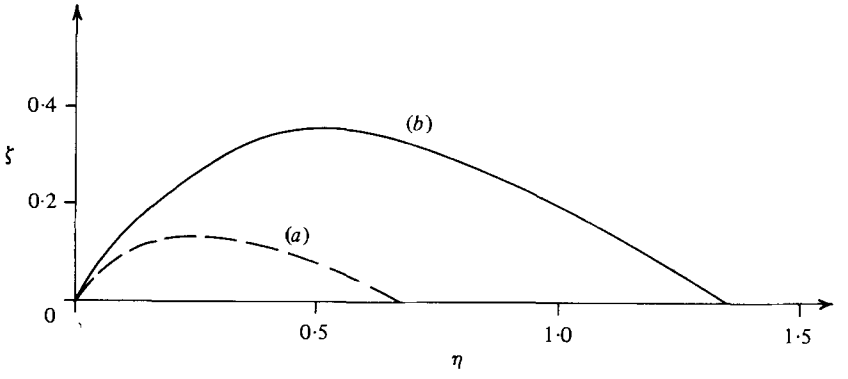

FIGURE 2. The body streamline for (a) $K = 2{\cdot}22$, $\beta = 0{\cdot}1$, $C = 2{\cdot}5$ (– – –) and for (b) $K = 1{\cdot}43$, $\beta = 0{\cdot}3$, $C = 0{\cdot}47$ (——).

The drag coefficient for one half of a symmetric body is taken as

$$C_D = \frac{\frac{1}{2}\mathscr{D}}{\frac{1}{2}\rho_0 U^2 hD}$$

and is equal to $(2\pi^4\beta^3/3h)\,C$. The results of our calculations are summarized in table 1 which gives the input parameters K, C, β and the computed height, length, aspect ratio (h/L), upstream velocities U_1, U_2, ratios of upstream velocities to obstacle heights U_1/h, U_2/h as well as the drag coefficient. We note that in table 1 the results for a given K were arranged in the order of increasing obstacle height. We further note that the lengths of our obstacles were always less than one half of the wavelength of the shortest lee wave present. This follows from the nature of our force distribution. If the obstacle were not closed at $\eta = \pi/\alpha_{\overline{K}}$, then it could not be closed in the downstream direction. Presumably a superposition of several planar force distributions located at different values of η could generate longer obstacles.

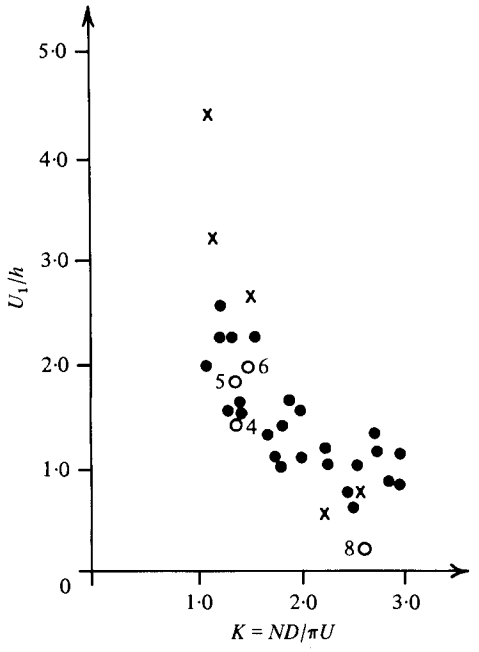

FIGURE 3. A diagram of U_1/h versus K, where the × 's are the present calculations, the ● 's are Baines' (1977) experimental values, and the ○'s are the observations of Wei *et al.* (1975). See text for explanation of numbers corresponding to (○)'s.

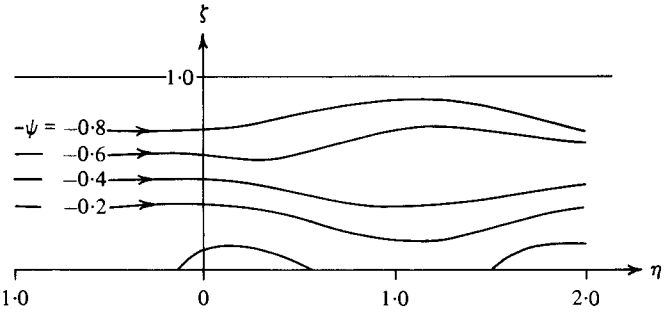

FIGURE 4. The streamline pattern for $K = 2{\cdot}22$ and $h = 0{\cdot}12$.

When $K = 1{\cdot}11$, we had the largest number of calculations. We can see that U_1 increases with h, although the rate of increase is somewhat less than linear (U_1/h decreases with increasing h). However, if we take $U_1/h = 4{\cdot}4$ for $K = 1{\cdot}11$, which is midway between the extremal values, less than 13 per cent variation of U_1/h with h is present. In figure 3, we plot U_1/h versus K (the × 's) using the mid-extremal values for each K, Baines' experimental results (the dots) and results taken from figures 4, 5, 6 and 8 of Wei *et al.* (the numbered circles). The values of h were not specified by Baines. Circles 4 and 8 are the results for a circular cylinder with h, the ratio of radius to channel depth, equal to 0·111 and aspect ratio, h/L, of 0·5. Circle 5 is for a circular cylinder with $h = 0{\cdot}056$, and circle 6 is for a vertical flat plate with $h = 0{\cdot}056$. For all these numbered cases the flow was separated in the lee of the obstacle. Since we would expect U_1/h to be a function of K, h, and h/L as well as the Reynolds number for blunt

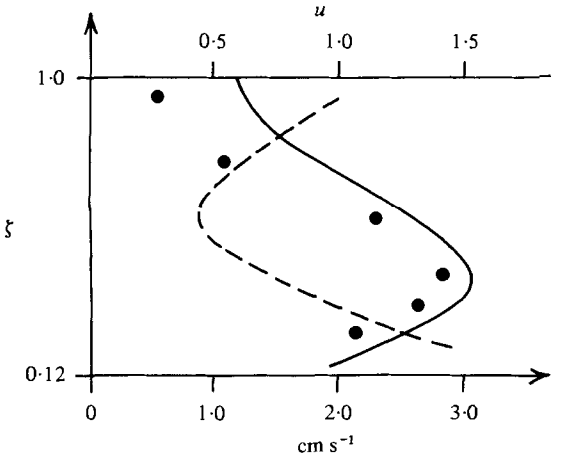

FIGURE 5. The horizontal velocity over the crest of an obstacle, experimental observations (●) and Long's model results (– – –) for $K = 2{\cdot}23$, $H = 0{\cdot}12$ from Baines (1977), where these values are referred to the lower scale. The solid line is our present results and should be referred to the upper scale.

obstacles, and there is variation in h and h/L between observed and calculated results, we can only say that U_1/h falls with K for both observed and calculated results.

Baines presents several streamline patterns. In figure 4, we present the calculated streamline pattern for $K = 2{\cdot}22$ with $h = 0{\cdot}122$. This is quite similar to Baines' figure 2(*a*) with $h = 0{\cdot}12$, $K = 2{\cdot}39$. However, the qualitative comparison of calculated and observed streamline patterns means little as there may be reasonable qualitative agreement but poor quantitative agreement.

The last point of comparison we can make is between the horizontal velocity measured by Baines over the crest of the obstacle, his calculation of that predicted by Long's model, and our calculation based on the Oseen model. In figure 5 we present Baines' results, which should be referred to the lower (absolute) horizontal scale, and our results, which should be referred to the upper (dimensionless) scale. The experimental and Long's model values have $K = 2{\cdot}23$, $h = 0{\cdot}12$ and our calculations have $K = 2{\cdot}22, h = 0{\cdot}122$. As we can see the agreement is quite good. We note that $h = 0{\cdot}122$ is the smallest barrier we generated and only this case could be compared with the measured profiles.

5. Limitations of the theory

It is clear from the preceding discussion that because of the differences in h and h/L between existing experimental and calculated results, as well as viscous effects which cause separation in the lee of blunt bodies, additional data will be necessary to confirm or refute the present theory. We now discuss some of the limitations of the theory and how they may be overcome.

First, the theory is inviscid. The body streamlines calculated from the theory are fairly streamlined so that boundary-layer separation should not occur. As long as boundary layers are thin compared with the obstacle height, an inviscid theory should apply. In practice this means that $(\nu T)^{\frac{1}{2}}/h' \ll 1$, where T is the towing time

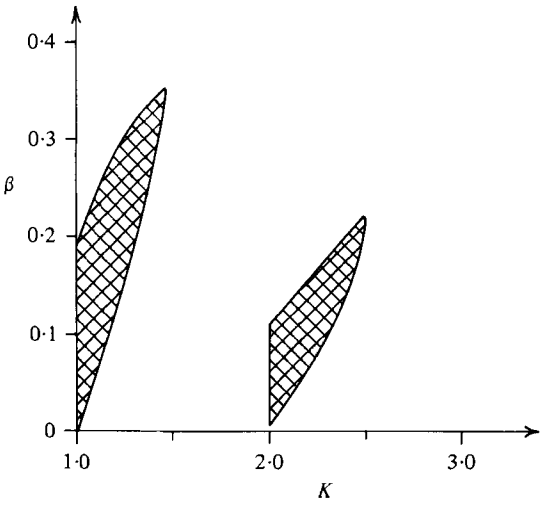

FIGURE 6. Values of K and β in cross-hatched areas have finite ranges for C leading to closed body streamlines for a parabolic force distribution.

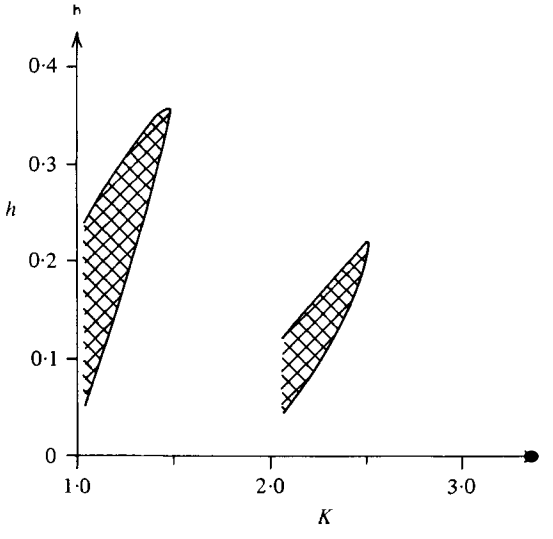

FIGURE 7. The cross-hatched areas indicate obstacle heights for body streamlines which may be computed for the parabolic force distribution.

necessary to establish a steady state with respect to a towed obstacle. The data of Wei *et al.* indicate that $T \sim 100/N$ so that $h' \gg 10(\nu/N)^{\frac{1}{2}}$.

A second limitation lies in the inverse nature of the solution and the result that every choice of β, C and K will not lead to a finite closed body streamline. In figure 6, any pair of values for β and K lying in the cross-hatched region will yield a range of C values for which closed body streamlines exist. This range of C values can be computed, with β and K chosen in the cross-hatched area, as indicated earlier, and with β, K and C specified, a body streamline can be computed. This body shape can then be tested experimentally to determine whether the theory is valid. From our calculations, table 1, we note that the aspect ratio $h/L = 0{\cdot}25$ exists for a range of K when

$\bar{K} = 1$. In figure 7, the range of computed dimensionless obstacle heights (the cross-hatched areas) is given versus K for the range of β values given in figure 6. For example, an obstacle with $h = 0{\cdot}25$ could be tested against the present theory for $1{\cdot}1 \leqslant K \leqslant 1{\cdot}4$.

It is hoped that the above discussion will enhance the utility of the theory.

6. Conclusions

We have determined the steady-state solution for the stratified flow over a bounded obstacle in a channel of finite height from the unsteady Oseen model by an inverse method. The limited comparisons made with the existing data suggest that this approach may be a viable alternative to Long's model for subcritical flows but additional experimental verification is necessary.

The author acknowledges the support of the National Science Foundation under Grant ATM78-16408 during the period in which this work was carried out.

REFERENCES

Baines, P. G. 1977 Upstream influence and Long's model in stratified flows. *J. Fluid Mech.* **82**, 147.

Janowitz, G. S. 1968 On wakes in stratified fluids. *J. Fluid Mech.* **33**, 417.

Janowitz, G. S. 1974 Line singularities in unbounded stratified flow. *J. Fluid Mech.* **66**, 455.

Lighthill, M. J. 1965 Group velocity. *J. Inst. Math. Applics* **1**, 1.

Lighthill, M. J. 1967 On waves generated in dispersive systems by travelling forcing effects, with applications to the dynamics of rotating fluids. *J. Fluid Mech.* **27**, 725.

Long, R. R. 1955 Some aspects of the flow of stratified fluids. III. Continuous density gradients. *Tellus* **7**, 343.

Trustrum, K. 1971 An Oseen model of the two-dimensional flow of a stratified fluid over an obstacle. *J. Fluid Mech.* **50**, 177.

Wei, S. N., Kao, T. W. & Pao, H. P. 1975 *Geophys. Fluid Dyn.* **6**, 315.

Wong, K. K. & Kao, T. W. 1970 Stratified flow over extended obstacles and its application to topographic effect on ambient wind shear. *J. Atmos. Sci.* **27**, 884.